Autophagy is the dominant type of programmed cell death in breast cancer MCF-7 cells exposed to AGS 115 and EFDAC, new sesquiterpene analogs of paclitaxel

Magdalena Górka[a], Włodzimierz M. Daniewski[b], Barbara Gajkowska[c], Elżbieta Łusakowska[d], Michał M. Godlewski[a] and Tomasz Motyl[a]

The molecular mechanism of cell death induced by AGS 115 and EFDAC, sesquiterpene analogs of paclitaxel, was investigated in human breast cancer MCF-7 cells. The study was carried out using laser scanning cytometry, homeostatic confocal microscopy, atomic force microscopy and electron microscopy. AGS 115 and EFDAC exhibited a microtubule-stabilizing effect as confirmed by a significant increase in α-tubulin aggregation. Both paclitaxel analogs also induced death in MCF-7 cells. Evaluation of biochemical and morphological features suggested that the major form of programmed cell death induced by AGS 115 and EFDAC was autophagy. This was confirmed by MAP I LC3 expression and the ultrastructural pattern revealed by electron microscopy. Surface images of cells undergoing autophagy showed that, unlike during apoptosis, the dimensions remained unchanged, but the surface of the cell was deformed. The occurrence of apoptosis was confirmed by the efflux of Smac/DIABLO from mitochondria, caspase-7 activation and DNA loss, and did not exceed 9.7%. Therefore, AGS 115 and EFDAC appear to be promising candidates for further investigation in anti-cancer therapy. *Anti-Cancer Drugs* **16:777–788**

Anti-Cancer Drugs 2005, **16:**777–788

Keywords: AGS 115, apoptosis, autophagy, EFDAC, sesquiterpene

[a]Department of Physiological Sciences, Faculty of Veterinary Medicine, Warsaw Agricultural University, Warsaw, Poland, [b]Institute of Organic Chemistry, [c]Department of Cell Ultrastructure, Medical Research Centre and [d]Institute of Physics, Polish Academy of Science, Warsaw, Poland.

Sponsorship: This work was performed in the frame of COST B20 Action: 'Mammary gland development, function and cancer' and was supported by grant 2 P06K 019 26 from the National Committee for Scientific Research, Poland.

Correspondence to T. Motyl, Department of Physiological Sciences, Faculty of Veterinary Medicine, Warsaw Agricultural University, Nowoursynowska 159, 02-776 Warsaw, Poland.
Tel/fax: +48 22 847 24 52;
e-mail: t_motyl@hotmail.com

Received 7 February 2005 **Revised form accepted** 4 May 2005

Introduction

Treatment of tumors with taxanes is reported to induce programmed cell death (PCD) followed by extensive karyokinesis resulting in endoreduplication [1]. However, many cancers are known to become resistant to taxanes following long-term treatment and side-effects may pose problems [2]. The most widely used taxanes in therapy are paclitaxel (taxol) and docetaxel (taxotere). The search for new drugs is focused on finding analogs of docetaxel and paclitaxel devoid of side-effects, but still possessing anti-tumor potential. Some of these drugs are already under clinical evaluation [3,4].

Various cell lines display complexity and variability in drug-induced apoptotic pathways. Both paclitaxel and docetaxel bind to the microtubule lattice [5–9], and impair cell mitosis [10] by elongation of the tubulin polymers into stabilized microtubule bundles [11]. This event initiates the apoptotic process after cell cycle arrest in pro-metaphase [12]. Unfortunately many cancers acquire resistance to microtubule-targeting drugs through (i) overexpression of drug efflux pumps such as P-glycoprotein that enhances efflux of the drug from the cell [13,14], (ii) point mutations in the genes encoding α- and β-tubulin that prevent binding of the drugs [15], and (iii) expression of different tubulin isoforms with impaired affinity for the drug [16,17].

The factors influencing apoptosis include Bcl family members, especially the anti-apoptotic proteins Bcl-2 and Bcl-x_L [18]. Disruption of microtubule structure by anti-microtubule drugs results in the inactivation of those anti-apoptotic proteins through phosphorylation [19,20]. Phosphorylation of Bcl-2 prevents formation of inactivating heterodimers with Bax and other death promoters from the Bcl-2 family, which directs cells towards apoptosis.

Docetaxel, derived semisynthetically by esterification of suitably protected 10-deacetyl baccatin III (10-DAB) with the side-chain, has a higher potency for microtubules because it accumulates in tumor cells to a greater extent than paclitaxel [21,22] and is retained for a longer period of time [23–26]. In some circumstances it may also be a more potent inducer of Bcl-2 phosphorylation

0959-4973

Fig. 1

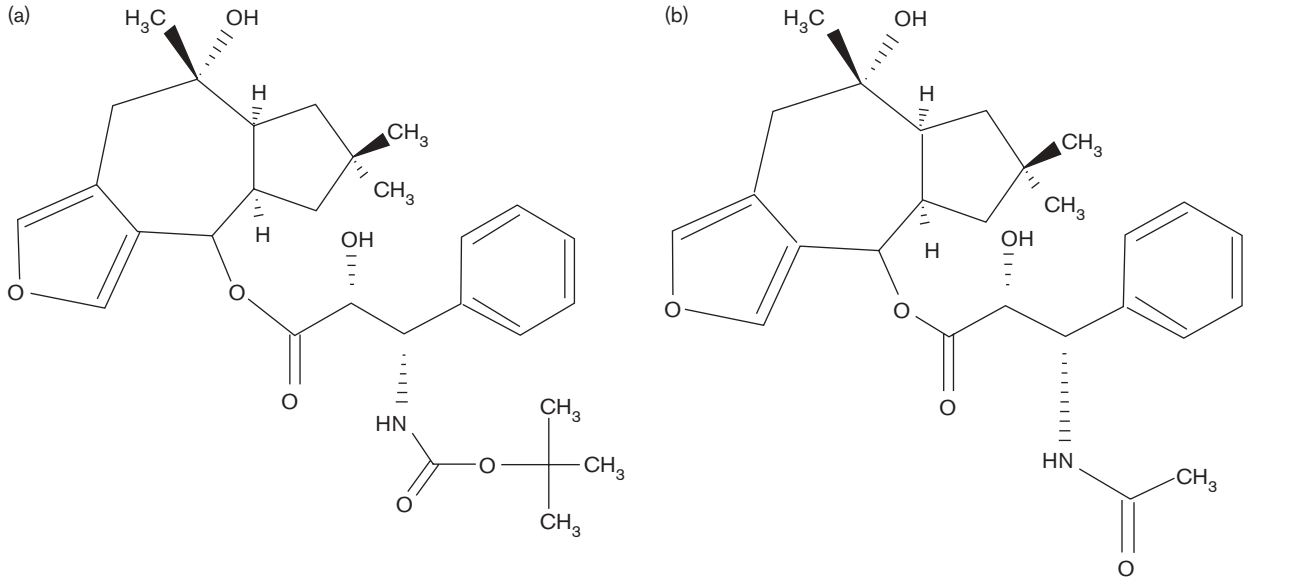

The sesquiterpenoic analogs of paclitaxel: AGS 115 (a) and (EFDAC) (b) synthesized by esterification of the sesquiterpenoic alcohol (4-epi-furandiol), isolated from mushrooms of *Lactarius* sp. and modified with suitably protected (2*R*,3*S*)-phenylisoserine. The combination of sesquiterpenoic alcohols with *N*-acylphenylisoserines expanded the biological properties of sesquiterpenes from anti-feedant and anti-viral towards anti-tumor activity.

[18,27]. Docetaxel is, therefore, used as first-line treatment of metastatic breast cancer and for patients with paclitaxel-resistant breast cancer [7,28].

N-Acylphenylisoserine side-chains are crucially important for the biological properties of drugs of the taxane family. The search for new anti-cancer drugs is focused on finding the analogs of taxanes possessing *N*-acylphenylisoserine side-chains attached to a sesquiterpene instead of a taxane [29]. The sesquiterpenoic analogs of paclitaxel were synthesized by esterification of sesquiterpenoic alcohols with suitably protected (2*R*,3*S*)-phenylisoserine followed by proper *N*-acylation (AGS 115 and EFDAC) [30,31]. This combination was expected to enhance the anti-tumor properties of sesquiterpenes. Preliminary experiments performed on several cancer cell lines and MO-MSV-induced tumors revealed promising cytostatic properties [32]. The present study was focused on examining the molecular mechanisms of cell death induced by two newly synthesized sesquiterpene analogs of paclitaxel, AGS 115 and EFDAC (Fig. 1), in breast cancer MCF-7 cells. Morphological and biochemical markers were used to distinguish apoptosis from autophagy using transmission electron microscopy (TEM), homeostatic confocal microscopy, atomic force microscopy (AFM), laser scanning cytometry (LSC) and Western blotting.

Methods

Media and reagents

DMEM powdered medium (without L-glutamine), L-glutamine, phosphate-buffered saline, pH 7.4 (PBS), fetal calf serum (FCS), fungizone, lipofectamine reagent, geneticin and gentamycin sulfate were obtained from Gibco/BRL (Paisley, UK). Polyclonal rabbit anti-α-tubulin, goat anti-MAP I LC3 and horseradish peroxidase-conjugated goat anti-chicken IgG were supplied by Santa Cruz Biotechnology (Santa Cruz, California, USA). Polyclonal rabbit anti-cleaved caspase-7 was purchased from Cell Signaling Technology (Beverly, Massachusetts, USA). Alexa Fluor 488 chicken anti-rabbit secondary antibody was purchased from Molecular Probes (Eugene, Oregon, USA). 7-Aminoactinomycin D (7-AAD) and MTT were purchased from Sigma (St Louis, Missouri, USA). The Magic Red Cathepsin Detection Kit was from ICN Biomedicals (Aurora, Ohio, USA). Sterile conical flasks, eight-chamber culture slides and sterile disposable pipettes were purchased from Nunc (Naperville, Illinois, USA). pDsRed2-Mito vector and pEGFP-N2 vector were obtained from BD Biosciences Clontech (Palo Alto, California, USA).

Cell culture

The human breast cancer MCF-7 cell line was obtained from the ATCC (Rockville, Maryland, USA). Cell cultures were maintained in DMEM supplemented with 10% (v/v) FCS, 0.2% (w/v) L-glutamine, 50 μg/ml

gentamycin, 2.5 μg/ml fungizone, 50 IU/ml penicillin and 50 μg/ml streptomycin in an atmosphere of 5% CO_2/95% humidified air at 37°C, and routinely subcultured every 2 or 3 days.

Drugs

AGS 115

(4R,4a*S*,7a*S*,8*S*)-6,6,8-trimethyl-4,4a,5,6,7,7a,8,9-octahydrocyclopenta[4,5]cyclohepta[1,2-*c*]-furan-4,8-diol 4-(*N*-tertbutoxycarbonyl-(2*R*,3*S*)-3-phenylisoserinate) (Fig. 1a) was prepared according to the procedure described by Sarosiek *et al.* [30].

EFDAC

(4R,4a*S*,7a*S*,8*S*)-6,6,8-trimethyl-4,4a,5,6,7,7a,8,9-octahydrocyclopenta[4,5]cyclohepta[1,2-*c*]-furan-4,8-diol 4-(*N*-acetyl-(2*R*,3*S*)-3-phenylisoserinate) (Fig. 1b) was prepared according to the procedure described by Barycki *et al.* [31].

MTT assay

MCF-7 cells were placed in 96-well plates at a density of 10 000 cells/well. AGS 115 and EFDAC stock solutions were diluted in medium, and added to the wells to achieve the desired final assay concentration. Cells were incubated at 37°C for 12 h, then 100 μl of MTT (2 mg/ml in PBS) was added to each well and incubated for an additional 4 h. Afterwards the medium was removed and the MTT formazan precipitate was dissolved in 100 μl of DMSO. The absorbance was measured at 570 nm in an Anthos 2010 microplate reader (Anthos Labtec, Wals, Austria).

Transfection

MCF-7 cells were transfected using lipofectamine reagent, pEGFP-Smac and pDsRed2-Mito vector. The construction of pEGFP-Smac was described previously [33]. The cells were incubated under optimal growth conditions until 70% confluency was achieved. Transfection solution was prepared combining 1.5 μg DNA diluted into 0.1 ml serum-free medium and 7 μl lipofectamine reagent diluted into 0.1 ml serum-free medium. The obtained mixture was incubated at room temperature for 30 min. The cells were then washed and overlaid with 0.8 ml serum-free medium, and transfection mixture was added dropwise and incubated at 37°C, under 5% CO_2 atmosphere for 3 h. Transfection medium was then exchanged with growth medium containing 10% FCS and incubation continued for 48 h following which transfected cells were selected using geneticin (400 μg/ml).

Western blot analysis

Cells were solubilized with ice-cold lysis buffer (pH 7.4) containing 1 mM Tris–HCl, 1% Triton X-100, 1 mM NaCl, 3 mM $MgCl_2$ 10 mM EDTA, 2 mM Na_3VO_4, 4 mM PMSF and 20 μg/ml leupeptin. Extracted proteins were removed by centrifugation at 10 000 *g* for 10 min. Aliquots of protein were electrophoretically separated on 12% SDS–polyacrylamide gels and transferred to nitrocellulose (Amersham Pharmacia Biotech, New Jersey, USA). Blocking was performed with a 5% w/v solution of non-fat powdered milk in TBST (pH 7.5) and 0.1% Tween 20. The membranes were probed with primary and secondary antibodies conjugated with horseradish peroxidase. Detection was performed with an ECL system and protein content determined using the Bradford method with bovine serum albumin (BSA) as a standard.

Experimental procedure for immunofluorescence staining

Exponentially growing cells were transferred to eight-chamber culture slides, cultured for 24 h and then incubated with the drugs dissolved in 10% FCS/DMEM for up to 6 h. The control cultures were treated with equivalent concentrations of DMSO suspended in 10% FCS/DMEM. Cells were then fixed in 0.25% formaldehyde for 15 min, washed twice with PBS, suspended in ice-cold 70% methanol and stored at 2°C for 30 min. The methanol was then aspirated and samples stored at −80°C until staining. To stain, cells were washed twice with PBS/1% BSA and incubated for 1 h with primary antibody diluted 1:250 with PBS/1% BSA. After primary incubation the cells were washed twice with PBS/1% BSA and incubated for an additional 1 h with 1:500 diluted secondary antibodies. The cells were then washed twice in PBS/1% BSA and finally incubated with 5 μg/ml 7-AAD for 30 min to counterstain the DNA. The chamber walls were then removed and coverslips mounted on the microscope slides using an anti-fade mounting medium (ICN Biomedicals) to permit examination.

LSC

Probes were analyzed by a LSC (CompuCyte, Boston, Massachusetts, USA) analyzing 5×10^3 or more cells per chamber area. Fluorescence excitation was provided by a 488-nm, 10-mW argon laser beam. The green fluorescence of Alexa Fluor 488-labeled antibody was measured using a combination of dichroic mirrors, filters transmitting at 520 ± 20 nm and far-red fluorescence of 7-AAD transmitting at above 650 nm. Aggregation of α-tubulin and caspase-7 [maximal pixel of fluorescence (MP)] was also measured. Results were analyzed using Excel (Microsoft, Redmond, Washington, USA).

AFM

AFM is used for studying surface properties of materials on an atomic scale of 100 μm and more using a probe with a very sharp tip (up to four atoms wide). Atomic forces between the sample and the tip cause changes of a distance between the tip and surface of the sample, and a

detector measures these changes. These data allow the computer to generate an accurate three-dimensional map of the surface topography. In our experiment we used the Multi Mode Scanning Probe Microscope (Digital Instruments, Santa Barbara, California, USA) set in Tapping Mode AFM with a spring constant of 26–57 N/m.

For AFM, the cells growing on coverslips were treated with drugs, fixed and stored in ice-cold methanol. Prior to analysis, the methanol was aspirated. All measurements were conducted during the 15 min after the cells were dried.

Confocal microscopy

Cells were visualized using a confocal laser scanning microscope FV-500 (Olympus, Warsaw, Poland). The combinations of excitation/emission were a HeNe 543-nm laser versus a 610-nm filter for MagicRed cathepsin substrate, and an argon 488-nm laser versus a 505–525-nm filter for α-tubulin and MAP I LC3. Three-dimensional images and cross-sections were reconstructed using the Fluoview program (Olympus).

Homeostatic confocal microscopy

Experiments conducted with living cells employed a confocal microscope equipped with a special homeostatic chamber (Solent Scientific, Portsmouth, UK) which allowed standard growing conditions for the cells over the experimental period (37°C, 5% CO_2, 95% humidified air). Transfected cells were cultured on coverglass-mounted, four-chamber culture slides. Cells were measured with the combination of excitation/emission using an argon 488-nm laser versus a 505–525-nm filter for GFP and a HeNe 543-nm laser versus a 610-nm filter for RFP. The experimental data were gathered from the series of cell cross-sections taken at 3-min intervals over 15 min. Drug was then added to the medium and cells were observed over the next 105 min.

TEM

The ultrastructural study of the MCF-7 cells required fixation in 0.1% glutaraldehyde and 4% paraformaldehyde in 0.1 M PBS for 1 h at 4°C. The cells were washed in PBS for 30 min, treated with 1% OsO_4 for 1 h, dehydrated in an ethanol gradient and then embedded in Epon. Ultrathin sections were cut with a diamond knife on a Reichert ultramicrotome, collected on copper grids, and stained with uranyl acetate and lead citrate. The sections were examined and photographed with a Joel 1200 XE electron microscope.

Statistical evaluation

The results were statistically evaluated by ANOVA and Tukey's multiple range tests using Microcal Origin version 5.0 (Microcal, Northampton, Massachusetts, USA) with $p \leq 0.05$ regarded as significant and $p \leq 0.01$ regarded as highly significant.

Fig. 2

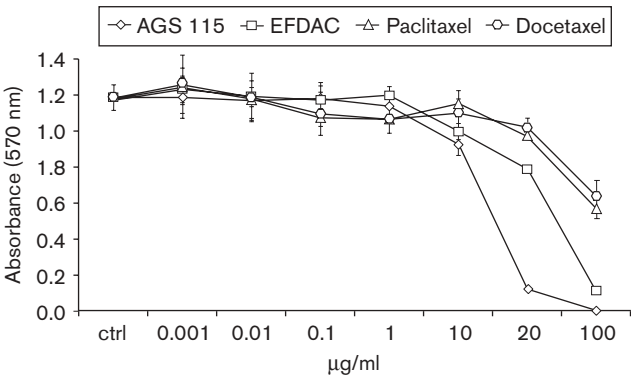

The viability of MCF-7 cells exposed to the examined drugs as evaluated with the MTT assay. Cells were exposed to various concentrations of drugs for 12 h. AGS 115 at 10 µg/ml caused 23% cell death and EFDAC at 20 µg/ml caused 34% cell death. Based on their effectiveness in inducing death in cancer cells, these drug concentrations were chosen for the next experiments. Each point represents the mean from five cultures.

Results

Viability of MCF-7 cells exposed to the new sesquiterpene analogs of paclitaxel

Cells were exposed to various concentrations of drugs for 12 h. The cytotoxicity of the drugs was determined using the MTT assay. Cells were exposed to both known taxanes (paclitaxel and docetaxel) and new sesquiterpene analogs (AGS 115 and EFDAC). The new agents acted more strongly than paclitaxel and docetaxel at the same concentration above 10 µg/ml (Fig. 2). After 12 h of culture, AGS 115 at 10 µg/ml caused a 23% decrease in MCF-7 cell viability and EFDAC at 20 µg/ml caused a 34% decrease in MCF-7 cell viability. Based on their effectiveness in inducing death in MCF-7 cancer cells, these concentrations of sesquiterpenes were chosen for additional study.

α-Tubulin aggregation in cells treated with sesquiterpene analogs and taxanes

Paclitaxel and docetaxel are anti-microtubule agents that stabilize tubulin polymerization and block microtubule disassembly in cells. Confocal microscopy was employed to evaluate the changes occurring at the tubulin cytoskeleton level. After 6 h of treatment with the examined agents, breast cancer MCF-7 cells were labeled with 7-AAD (DNA) and α-tubulin antibody conjugated with fluorochrome. In the control, non-stimulated cells, tubulin-related green fluorescence was uniformly arranged within the tumor cells (Fig. 3a). Administration of the drugs to the incubation medium induced the

Fig. 3

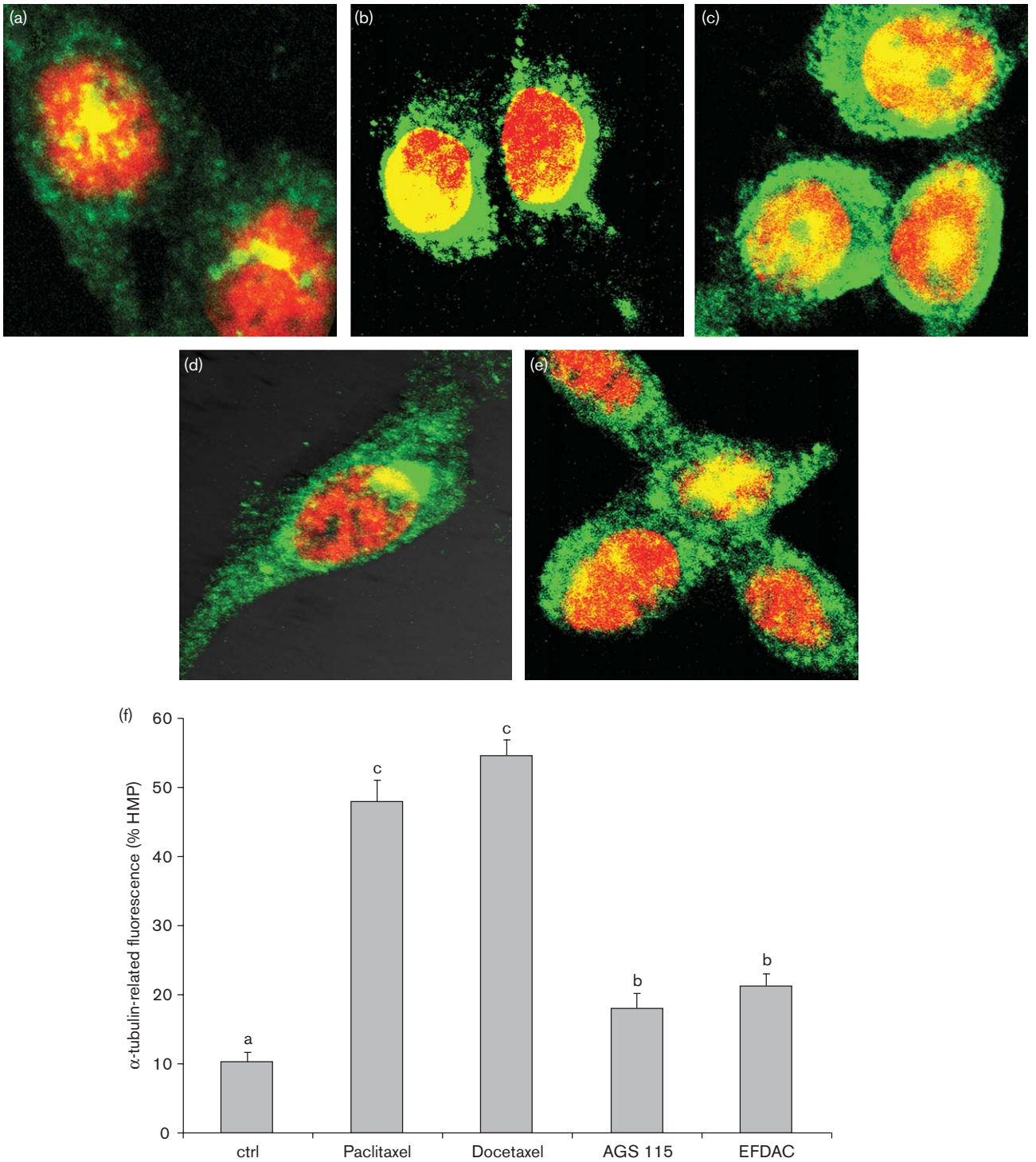

α-Tubulin aggregation in cells treated for 6 h with the examined compounds. Microphotographs of MCF-7 control cells (a), and cells treated with paclitaxel (b), docetaxel (c), AGS 115 (d) and EFDAC (e). In drug-treated cells (b–e), the increase of α-tubulin-related green fluorescence was clearly visible. (f) Changes in the aggregation of α-tubulin in MCF-7 cells treated with the examined agents, measured by LSC. The '% HMP' refers to the number of cells with the highest value of protein-related fluorescence. The drug treatment significantly increased the aggregation of α-tubulin in the case of paclitaxel and docetaxel, and to a lower extent in the case of AGS 115 and EFDAC. Drugs were applied in the following concentrations: 10 μg/ml AGS 115, paclitaxel and docetaxel, and 20 μg/ml EFDAC. Means (±SD) bearing different superscripts differ significantly ($p \leq 0.05$).

aggregation of α-tubulin, manifested by a higher intensity of green fluorescence within the cells (Fig. 3b–e).

Similar results were obtained by LSC in terms of the number of cells with a high aggregation (high MP) of α-tubulin-related fluorescence (Fig. 3f). The drug treatment significantly ($p \leq 0.01$) increased the aggregation of α-tubulin with paclitaxel (from 7.8% in the control to 39.5%) and docetaxel (44.5%). AGS 115 and EFDAC increased the aggregation of α-tubulin to a lesser, but still significant ($p \leq 0.05$), extent (14.4 and 17.2%, respectively).

Apoptotic effects of AGS 115 and EFDAC in MCF-7 cells

In order to determine whether the new compounds induced apoptosis, DNA content and caspase-7 activation were analyzed. LSC showed that drug treatment increased the apoptotic ratio (number of cells in the sub-G_1 area of the DNA histogram) from 2.6% in the control to 6.1% in the case of AGS 115 and 9.7% in the case of EFDAC after 6 h of incubation (Fig. 4a). A lower number of apoptotic cells was observed in the case of paclitaxel (4%) and docetaxel (3.7%) treatment.

The level of active caspase-7 (the major caspase involved in the degradation phase of apoptosis in MCF-7 cells) was analyzed by Western blotting. The experiment revealed that an increase in the level of active caspase-7 content in the treated cells was time dependent (Fig. 4b). To confirm these results, the level of activated caspase-7 was also analyzed by LSC. LSC analysis revealed similar results, although the increase in caspase-7 was greater after AGS 115 treatment (Fig. 4c). The percentage of cells with high fluorescence was elevated by 27.5% in AGS 115-tretaed cultures and by 16.5% in EFDAC-treated cultures following 12 h of incubation.

Four-dimensional (three-dimensional/time) homeostatic confocal microscopy was used to study the kinetics of Smac/DIABLO release from mitochondria in breast

Fig. 4

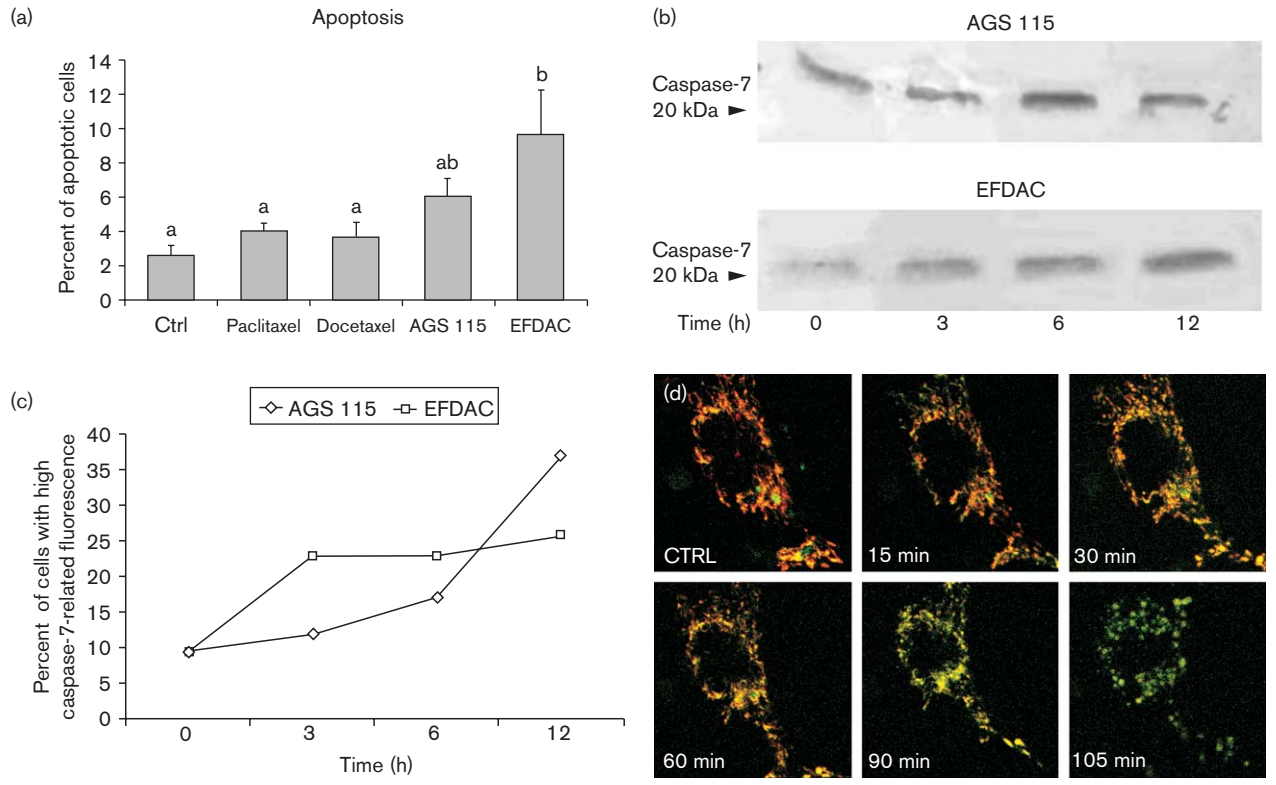

(a) LSC analysis of DNA content in the sub-G_1 area of the DNA histogram, representing apoptotic cells. The highest percentage of treated cells in the sub-G_1 area was observed in the case of EFDAC (9.7%) and AGS 115 (6.1%). The low number of cells in the sub-G_1 area observed in cultures treated with the examined compounds was a result of the specificity of the death-inducing effect of these drugs, which is associated with autophagy rather than apoptosis. (b) Western blot analysis of active caspase-7 levels in MCF-7 cells treated with AGS 115 and EFDAC. (c) LSC analysis of active caspase-7 expression in AGS 115- and EFDAC-treated MCF-7 cells. (d) Four-dimensional (three-dimensional/time) homeostatic confocal microscopy analysis of Smac/DIABLO efflux form mitochondria of living AGS 115-treated MCF-7 cells. The Smac/DIABLO efflux was visible as an increase of green GFP-related fluorescence present in the cell after 90 min of cell exposure to the drug. Drugs were applied in the following concentrations: 10 μg/ml AGS 115, paclitaxel and docetaxel, and 20 μg/ml EFDAC. Means (± SD) bearing different superscripts differ significantly ($p \leq 0.05$).

cancer MCF-7 cells treated with AGS 115. Smac/DIABLO, the second mitochondria-derived activator of caspases, is a pro-apoptotic protein released from the mitochondrial intermembrane space during apoptosis. It promotes caspase activation by neutralization of IAP caspase-binding domains [33]. The breast cancer MCF-7 cell line was transfected twice with Smac/DIABLO-GFP and mitovector-RFP. Mitovector-RFP is a protein of mitochondrial localization emitting red fluorescence. In the untreated cell, Smac/DIABLO-GFP-related fluorescence (green) overlaid the mitochondria-derived red fluorescence (Fig. 4d; ctrl). Administration of AGS 115 to the incubation medium resulted in an increase of green fluorescence within the cell, suggesting release of Smac/DIABLO from mitochondria following 90 min of cell exposure to the drug.

Effect of drugs on MAP I LC3 expression in MCF-7 cells

In addition to apoptosis, MCF-7 cells are able to trigger an alternative type of PCD, autophagy, which has been demonstrated in the case of tamoxifen [34,35] or camptothecin in Bid-deficient MCF-7 cells [36]. To evaluate the role of autophagy, MCF-7 cells were incubated with the examined drugs, and labeled with 7-AAD (DNA) and MAP I LC3 antibody (autophagosomes) (Fig. 5). MAP I LC3 was originally isolated as a small subunit of microtubule-associated protein [37], but is now believed to be the only reliable marker for autophagy, i.e. the lysosome-mediated form of cell death. This protein is necessary for formation of intermediate membrane structures that form the autophagosome [38]. The confocal microscopy images showed an increase in cell number with high green fluorescence in cultures treated with the newly synthesized taxanes (AGS 115 and EFDAC) (Fig. 5d and e) and reference drugs (paclitaxel and docetaxel) (Fig. 5b and c). To perform quantitative analysis of MAP I LC3 expression, confocal images were calculated by the MicroImage System (Olympus) (Fig. 5f). Increments of MAP I LC3 protein were presented by the increase in the ratio of the integrated optical density (IOD) of protein fluorescence to DNA area (Fig. 5f). The MAP I LC3 IOD to DNA area ratio was employed to avoid differences in IOD values resulting from variable cell numbers in the acquired confocal images. This ratio rose by 30-fold in cells treated with docetaxel and its analog AGS 115, by 15-fold in the case of paclitaxel, and by 12-fold in the case of its analog EFDAC.

Surface image of cells undergoing apoptosis and autophagy induced by AGS 115 and EFDAC

Distortion of the cytoskeleton is reflected by the shape and surface pattern of the cell. AFM enabled precise cell imaging and reconstruction of the surface image. A representative, control cell is presented on Fig. 5(a) with a barely visible rim around the nucleus ('nucleus crater'). During apoptosis, the cell condensed from 29.3 to 21.5 μm and the 'nuclear crater' disappeared (Fig. 6b). In cells undergoing autophagy the dimensions of the cells remained unchanged, but the depth of the 'nuclear craters' increased from 110 nm in controls to 292 nm in AGS 115 (Fig. 6c) and 702 nm in EFDAC (Fig. 6d). The observed surface of the cells was deformed, which together with the sinking of the nucleus suggested partial degradation of the cytoskeleton and loss of nuclear scaffolding.

Ultrastructural features of autophagy in cells treated with AGS 115 and EFDAC

The ultrastructural changes in the cells during AGS 115 and EFDAC treatment were evaluated with the use of TEM. The untreated cells exhibited the correct ultrastructural morphology (Fig. 7a and e). The uniform nuclei were composed of finely dispersed chromatin and one or two nucleoli. The cytoplasm was filled with polyribosomes, rough endoplasmic reticulum and abundant mitochondria of various shapes. The Golgi complexes were located in the cytoplasm at the periphery of the nucleus. A small number of lysosomes and dense bodies were also visible.

Treatment with the examined compounds resulted in the formation of giant autophagosomes, and the sequestration of cytoplasm portions and organelles by double membranes derived from the endoplasmic reticulum (Fig. 7b, c, f and g). A double-membraned giant autophagosome filled with organelles, multilamellar bodies and electron dense material was observed in cells treated with EFDAC (Fig. 7g, arrow). In the final stage, the MCF-7 cells exhibited loss of plasma membrane integrity and intensive cytoplasm vacuole formation. No organelles and autophagic vacuoles could be identified in these cells, only the well-preserved pyknotic nuclei (Fig. 7d and h).

These processes precede nuclear and cytoskeletal destruction. Intermediate filaments and microfilaments were largely preserved; presumably, the cytoskeleton was required for autophagocytosis.

Discussion

Sesquiterpenoic alcohols isolated from *Lactarius* sp. mushrooms exhibit anti-feedant and anti-viral properties [29,39,40]. Modification of these alcohols by esterification of the hydroxyl groups with *N*-acylphenylisoserine produces some anti-cancer activity [30]. It is known that *N*-acylphenylisoserine chains are of crucial importance for the biological properties of anti-tumor drugs possessing taxane skeletons (paclitaxel and docetaxel). The effectiveness of taxanes in combination chemotherapy for advanced breast cancer has been well described [41–45].

Fig. 5

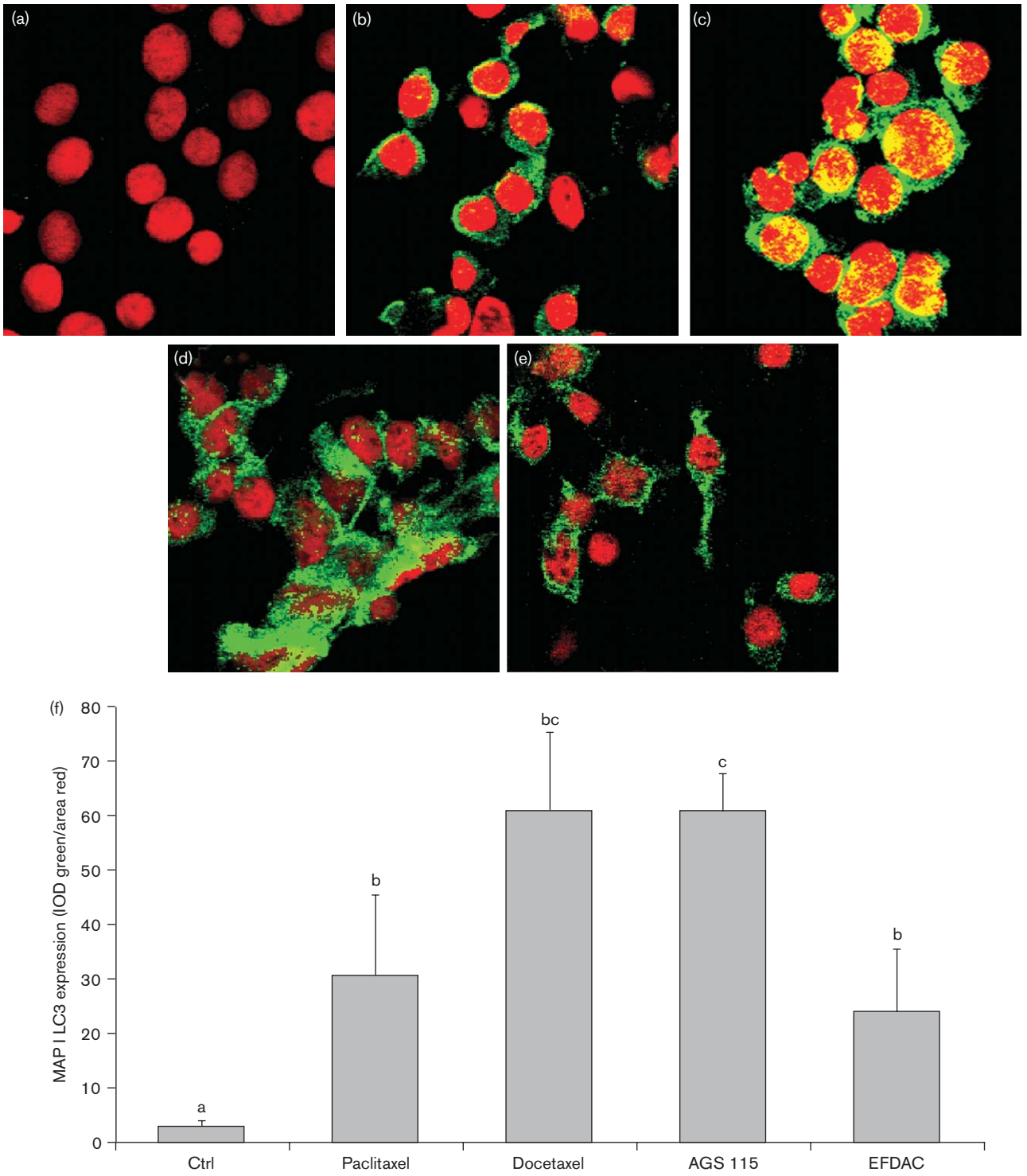

MAP I LC3 expression in MCF-7 cells treated with control (a), paclitaxel (b), docetaxel (c), AGS 115 (d) and EFDAC (e). MAP I LC3 is believed to be the only reliable marker for autophagy, i.e. the lysosome-mediated form of cell death. All examined compounds increased the MAP I LC3 expression with the highest level observed in docetaxel- and AGS 115-treated cultures (c and d, respectively). (f) To perform quantitative analysis of MAP I LC3 expression, confocal images were calculated by the MicroImage System. Increase of MAP I LC3 protein was presented by the increase in the ratio of the IOD of protein fluorescence to DNA area. Drugs were applied in the following concentrations: 10 μg/ml AGS 115, paclitaxel and docetaxel, and 20 μg/ml EFDAC. Means (± SD) bearing different superscripts differ significantly ($p \leq 0.05$).

Fig. 6

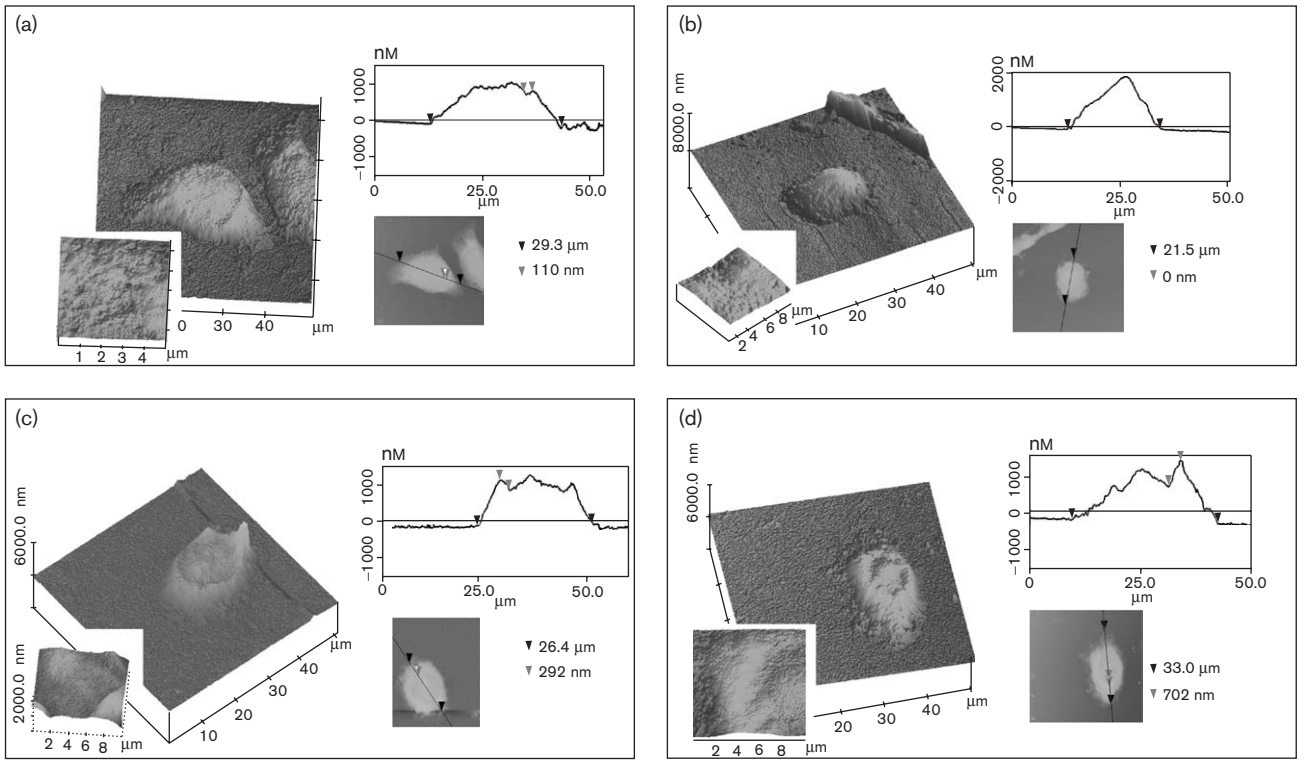

The surface images of MCF-7 cells treated for 6 h with the examined compounds and their cross-sections acquired by AFM. The representative control cell (a) shows a barely visible rim around the nucleus ('nucleus crater'). During apoptosis the cell shrinks, the cytoplasm condenses and the 'nuclear crater' disappears (b). In cells undergoing autophagy the dimensions of the cells remained unchanged, but the 'nuclear crater' depth increased in cells treated with AGS 115 (c) and EFDAC (d), suggesting a partial loss of cytoskeleton integrity and nucleus scaffolding.

The present study focused on the mechanism of PCD induced by AGS 115 and EFDAC in human breast cancer MCF-7 cells in culture. Our results revealed that the dominant type of PCD-induced by AGS 115 and EFDAC was autophagy (PCD type II), as demonstrated by analysis of specific morphological and biochemical features of apoptosis and autophagy.

Both compounds decreased cell viability as measured by the MTT test (Fig. 2). In the case of AGS 115, this effect was even stronger than in paclitaxel- or docetaxel-treated cultures. Stabilization of microtubules is the biochemical feature which precedes PCD induced by taxanes [46]. This effect was observed in cell cultures treated with paclitaxel and docetaxel, as well as with AGS 115 and EFDAC (Fig. 3). The presented results demonstrate that both sesquiterpene analogs studied are microtubule-interacting substances with a lower effectiveness than taxanes. Conversely, the apoptotic effect of these sesquiterpenes, as measured by DNA loss, was greater than observed with the taxanes. Caspase-3 is not expressed in the MCF-7 cell line [47,48]. As a result, the main caspases in this cell line are caspase-6 and -7. Our experiments suggested that the level of the active (cleaved) form of caspase-7 was the most reliable biochemical marker for apoptosis (PCD type I) (Fig. 4b). LSC revealed that the increase in cell numbers with elevated active caspase-7 did not exceed 30 and 20% after 12 h of cell culture exposure to AGS 115 and EFDAC, respectively (Fig. 4c). Fewer apoptotic cells were observed when DNA content was used as a criterion for apoptosis (Fig. 4a). Based on these results, we assumed that the majority of MCF-7 cells were resistant to apoptosis induced by sesquiterpenes. However, cell subpopulations sensitive to apoptotic signals existed and triggered PCD type I via the mitochondrial pathway, as demonstrated by the release of Smac/DIABLO from mitochondria (Fig. 4d). Smac/DIABLO activates executory caspases by their release from the inhibitory effect of IAPs [33]. The release of Smac/DIABLO from mitochondria occurred within 2 h of drug exposure and preceded any morphological findings of apoptosis (Fig. 4d).

Autophagy (PCD type II) is the dominant type of MCF-7 cell death induced by AGS 115 and EFDAC. Autophagy is biochemically and morphologically distinct

Fig. 7

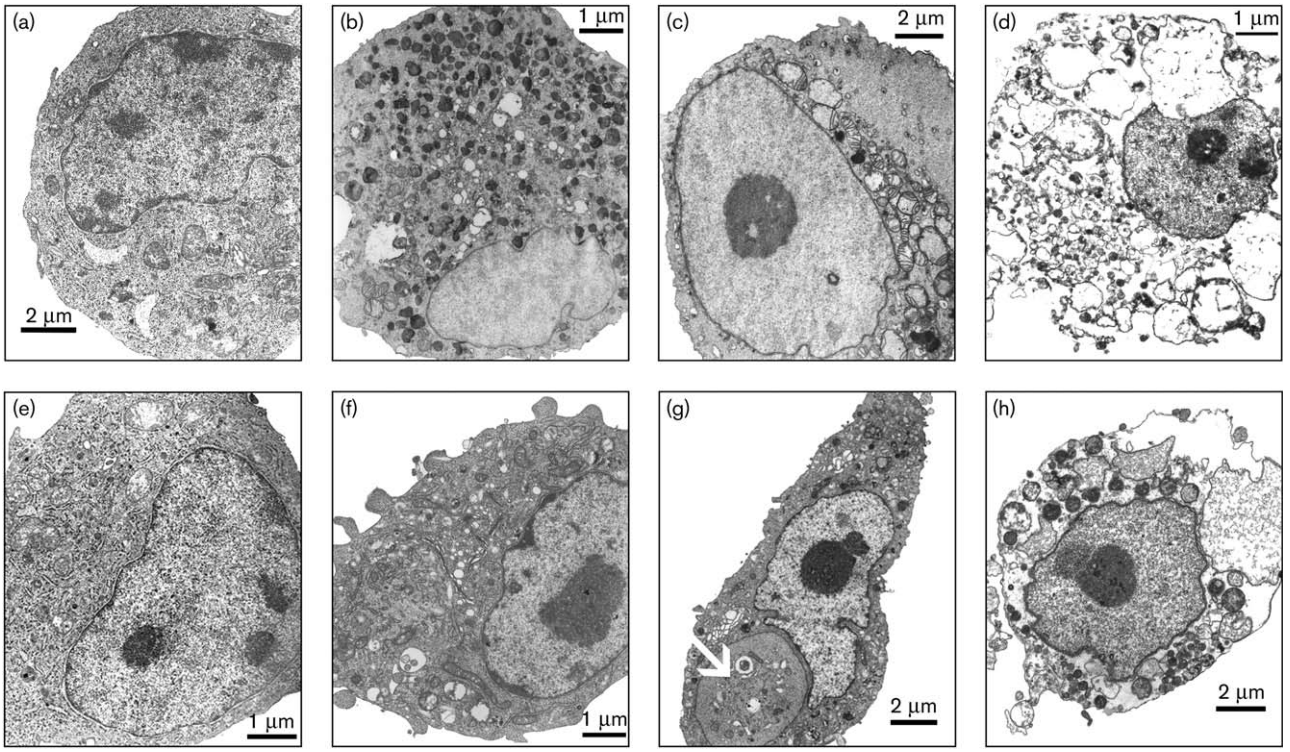

A series of microphotographs showing MCF-7 cells treated with AGS 115 (a–d) and EFDAC (e–h) obtained by TEM. The untreated cells exhibited the correct ultrastructural morphology (a and e). After AGS 115 and EFDAC treatment, cells presented an oval or irregular nuclei, with deep invaginations of the nuclear envelope, clear, dispersed chromatin and an electron-dense nucleus. The loss of the endoplasmic reticulum and Golgi complex was visible, and the cytoplasm contained only swollen mitochondria in the perinuclear area, ribosomes, lysosomes and autophagic vacuoles of various dimensions (b, c, f and g). The cytoplasm contained a variety of autophagic vacuoles at several stages, including a double-membraned giant autophagosome (g, arrow) filled with organelles, multilamellar bodies and electron-dense material. In the final stage, the MCF-7 cells exhibited loss of plasma membrane integrity and intensive cytoplasm vacuolization (d and h). The cells were treated with the examined compounds for: 3 (b and f), 6 (c and g) and 12 h (d and h); a and e = untreated control cells.

from apoptosis, is controlled by a different set of genes [49–51], and malignant transformation is frequently associated with suppression of autophagy [52]. The recent implication of tumor suppressors like beclin 1, DAP kinase and PTEN in the autophagic pathway suggests a relationship between autophagy deficiency and carcinogenesis [52].

The ability to induce autophagy in cancer cells could be especially important in apoptosis-resistant cell lines, when pro-apoptotic genes were mutated. A recent study performed in our laboratory revealed that silencing of the pro-apoptotic gene *bid* in MCF-7 cells leads to the inhibition of apoptosis and to a shift of cell death towards autophagy [36]. It is postulated that autophagic cell death induction by some anti-cancer agents underlines their potential in a new cancer therapy modality [52]. Our study proved that the new sesquiterpene analogs of paclitaxel, AGS 115 and EFDAC, were capable of inducing autophagy with its characteristic biochemical and morphological features. The most typical biochemical feature of autophagy induced by AGS 115 and EFDAC was increased expression of MAP I LC3 (Fig. 5), currently regarded as the only reliable marker of autophagosome formation [38,53]. Although MAP I LC3 exists on the autophagosome membrane, it was first discovered as a protein binding to microtubules [37]. It may suggest an involvement of microtubules in the mechanism of the autophagic form of cell death induced by microtubule-stabilizing drugs. It has been shown that destabilization of microtubules by either vinblastine or nocodazole blocks the maturation of autophagosomes, whereas their stabilization by paclitaxel increases the fusion between autophagosomes and lysosomes [54]. In the present study the highest expression of MAP I LC3 was observed in the case of AGS 115 and docetaxel (Fig. 5), which may suggest that the side-chain represented by *N*-tert-butoxycarbonyl-(2*R*,3*S*)-phenylisoserine facilitates the induction of autophagy in breast cancer MCF-7 cells.

In contrast to apoptosis, the shape and size of autophagic cells remained unchanged (Fig. 6), which indicates

preservation of the cytoskeleton. However, the nuclei dipped, forming the 'crater' on the cell surface, which was probably associated with partial disintegration of actin microfilaments. At the ultrastructural level, electron micrographs showed swelling of endoplasmic reticulum channels, multiplication of lysosomes, formation of autophagolysosomes and hyperactivation of the nucleolus (Fig. 7). Different stages of autophagolysosomes were observed: an early stage containing visible organelles, a middle stage with a condensed structure containing organelles and myelin figures, and a late stage with large, electron-empty vacuoles, sometimes containing myelin remnants or residual material.

In conclusion, sesquiterpene analogs of paclitaxel are promising candidates for a new approach in anti-cancer therapy. They exhibit a microtubule-stabilizing effect and are able to induce PCD dominated by autophagy (PCD type II) in human breast cancer MCF-7 cells.

References

1 Makarovskiy AN, Siryaporn E, Hixson DC, Akerley W. Survival of docetaxel-resistant prostate cancer cells *in vitro* depends on phenotype alterations and continuity of drug exposure. *Cell Mol Life Sci* 2002; **59**:1198–1211.

2 Drukman S, Kavallaris M. Microtubule alterations and resistance to tubulin-binding agents. *Int J Oncol* 2002; **21**:621–628.

3 Jordan MA, Ojima I, Rosas F, Distefano M, Wilson L, Scambia G, *et al.* Effects of novel taxanes SB-T-1213 and IDN5109 on tubulin polymerization and mitosis. *Chem Biol* 2002; **9**:93–101.

4 Baloglu E, Miller ML, Roller EE, Cavanagh EE, Leece BA, Goldmacher VS, *et al.* Synthesis and biological evaluation of novel taxoids designed for targeted delivery to tumors. *Bioorg Med Chem Lett* 2004; **14**:5885–5888.

5 Manfredi JJ, Parness J, Horwitz SB. Taxol binds to cellular microtubules. *J Cell Biol* 1982; **94**:688–696.

6 Rao S, Horwitz SB, Ringel I. Direct photoaffinity labeling of tubulin with taxol. *J Natl Cancer Inst* 1992; **84**:785–788.

7 Valero V, Jones SE, Von Hoff DD, Booser DJ, Mennel RG, Ravdin PM, *et al.* - A phase II study of docetaxel in patients with paclitaxel-resistant metastatic breast cancer. *J Clin Oncol* 1998; **16**:3362–3368.

8 Ringel I, Horwitz SB. Effect of alkaline pH on taxol–microtubule interactions. *J Pharmacol Exp Ther* 1991; **259**:855–860.

9 Diaz JF, Andreu JM. Assembly of purified GDP-tubulin into microtubules induced by taxol and taxotere: reversibility, ligand stoichiometry, and competition. *Biochemistry* 1993; **32**:2747–2755.

10 Long BH, Fairchild CR. Paclitaxel inhibits progression of mitotic cells to G_1 phase by interference with spindle formation without affecting other microtubule functions during anaphase and telephase. *Cancer Res* 1994; **54**:4355–4361.

11 Schiff PB, Fant J, Horwitz SB. Promotion of microtubule assembly *in vitro* by taxol. *Nature* 1979; **277**:665–667.

12 Rowinsky EK. The development and clinical utility of the taxane class of antimicrotubule chemotherapy agents. *Annu Rev Med* 1997; **48**:353–374.

13 Mechetner EB, Schott B, Morse BS, Stein WD, Druley T, Davis KA, *et al.* P-glycoprotein function involves conformational transitions detectable by differential immunoreactivity. *Proc Natl Acad Sci USA* 1997; **94**: 12908–12913.

14 Krishna R, Mayer LD. The use of liposomal anticancer agents to determine the roles of drug pharmacodistribution and P-glycoprotein (PGP) blockade in overcoming multidrug resistance (MDR). *Anticancer Res* 1999; **19**:2885–2891.

15 Giannakakou P, Sackett DL, Kang YK, Zhan Z, Buters JT, Fojo T, *et al.* Paclitaxel-resistant human ovarian cancer cells have mutant beta-tubulins that exhibit impaired paclitaxel-driven polymerization. *J Biol Chem* 1997; **272**:17118–17125.

16 Burkhart CA, Kavallaris M, Band Horwitz S. The role of beta-tubulin isot ypes in resistance to antimitotic drugs. *Biochim Biophys Acta* 2001; **1471**:O1–O9.

17 Ranganathan S, Dexter DW, Benetatos CA, Hudes GR. Cloning and sequencing of human betaIII-tubulin cDNA: induction of betaIII isotype in human prostate carcinoma cells by acute exposure to antimicrotubule agents. *Biochim Biophys Acta* 1998; **1395**:237–245.

18 Stein CA. Mechanisms of action of taxanes in prostate cancer. *Semin Oncol* 1999; **26**:3–7.

19 Kolfschoten GM, Hulscher TM, Duyndam MC, Pinedo HM, Boven E. Variation in the kinetics of caspase-3 activation, Bcl-2 phosphorylation and apoptotic morphology in unselected human ovarian cancer cell lines as a response to docetaxel. *Biochem Pharmacol* 2002; **63**:733–743.

20 Basu A, Haldar S. Identification of a novel Bcl-x_L phosphorylation site regulating the sensitivity of taxol- or 2-methoxyestradiol-induced apoptosis. *FEBS Lett* 2003; **538**:41–47.

21 Ringel I, Horwitz SB. Studies with RP 56976 (taxotere): a semisynthetic analogue of taxol. *J Natl Cancer Inst* 1991; **83**:288–291.

22 Riou JF, Naudin A, Lavelle F. Effects of Taxotere on murine and human tumor cell lines. *Biochem Biophys Res Commun* 1992; **187**:164–170.

23 Michaud LB, Valero V, Hortobagyi G. Risks and benefits of taxanes in breast and ovarian cancer. *Drug Safety* 2000; **23**:401–428.

24 Leahy M, Howell A. Docetaxel. *Br J Hosp Med* 1997; **57**:141–144.

25 Hortobagyi GN. Recent progress in the clinical development of docetaxel (Taxotere). *Semin Oncol* 1999; **26**:32–36.

26 Consolini R, Pui CH, Behm FG, Raimondi SC, Campana D. *In vitro* cytotoxicity of docetaxel in childhood acute leukemias. *J Clin Oncol* 1998; **16**:907–913.

27 Haldar S, Basu A, Croce CM. Bcl2 is the guardian of microtubule integrity. *Cancer Res* 1997; **57**:229–233.

28 Verweij J, Clavel M, Chevalier B. Paclitaxel (Taxol) and docetaxel (Taxotere): not simply two of a kind. *Ann Oncol* 1994; **5**:495–505.

29 Kopczacki P, Gumułka M, Masnyk M, Grabarczyk H, Nowak G, Daniewski WM. Synthesis and antifeedant properties of *N*-benzoylphenylisoserinates of *Lactarius* sesquiterpenoid alcohols. *Phytochemistry* 2001; **58**:775–787.

30 Sarosiek A, Masnyk M, Gumułka M, Daniewski WM, Kobus M, Krawczyk E, *et al.* Synthesis and cytotoxic properties of *N*-Boc-phenylisoserinates of sesquiterpenoic alcohols from mushrooms of *Lactarius* genus, as analogs of taxotere. *Polish J Chem* 2002; **76**:73–82.

31 Barycki R, Gumułka M, Masnyk M, Daniewski WM, Kobus M, Łuczak M. Synthesis of *N*-acetyl-3-phenylisoserinates of sesquiterpenoid alcohols of *Lactarius* origin. *Collect Czech Chem Commun* 2002; **67**:75–82.

32 Kobus M, Przybylski M, Łuczak M, Krawczyk E, Kopczacki P, Daniewski W. An *in vitro* and *in vivo* evaluation of antiviral and cytostatic activity of *N*-benzoylphenylisoserinates of sesquiterpenes–analogs of taxol. In: *Proc 12th Mediterranean Cong Chemotherapy*, Marakesh; 2000, pp. 141–147.

33 Górka M, Godlewski MM, Gajkowska B, Wojewódzka U, Motyl T. Kinetics of Smac/DIABLO release from mitochondria during apoptosis of MCF-7 breast cancer cells. *Cell Biol Int* 2004; **28**:741-754.

34 Bursch W, Hochegger K, Torok L, Marian B, Ellinger A, Hermann RS. Autophagic and apoptotic types of programmed cell death exhibit different fates of cytoskeletal filaments. *J Cell Sci* 2000; **113**:1189–1198.

35 Scarlatti F, Bauvy C, Ventruti A, Sala G, Cluzeaud F, Vandewalle A, *et al.* Ceramide-mediated macroautophagy involves inhibition of protein kinase B and up-regulation of beclin 1. *J Biol Chem* 2004; **279**:18384–18391.

36 Lamparska-Przybysz M, Gajkowska B, Motyl M. Apoptosis and autophagy depend on cathepsin activation in breast cancer MCF-7 cells. Presented at: *5th Interdisciplinary Conf on Mechanisms of Cell Death and Disease: Advances in Therapeutic Intervention and Drug Development,* Cascais; 2004.

37 Mann SS, Hammarback JA. Molecular characterization of light chain 3. A microtubule binding subunit of MAP1A and MAP1B. *J Biol Chem* 1994; **269**:11492–1147.

38 Kabeya Y, Mizushima N, Ueno T, Yamamoto A, Kirisako T, Noda T, *et al.* LC3, a mammalian homologue of yeast Apg8p, is localized in autophagosome membranes after processing. *EMBO J* 2000; **19**:5720–5728.

39 Daniewski WM, Gumułka M, Ptaszyńska K, Skibicki P, Błoszyk E, Drożdż B, *et al.* Antifeedant activity of some sesquiterpenoids of the genus *Lactarius*. *Eur J Entemol* 1993; **90**:65–70.

40 Daniewski WM, Gumułka M, Przesmycka D, Ptaszyńska K, Błoszyk E, Drozdz B. Sesquiterpenes of lactarius origin, antifeedant activity structure relationship. *Phytochemistry* 1995; **38**:1161–1168.

41 Okawa Y, Sugiyama K, Aiba K, Hirano A, Uno S, Hagino T, *et al.* Successful combination therapy with trastuzumab and Paclitaxel for adriamycin- and docetaxel-resistant inflammatory breast cancer. *Breast Cancer* 2004; **11**:309–312.

42 Glynn SA, Gammell P, Heenan M, O'Connor R, Liang Y, Keenan J, *et al.* A new superinvasive *in vitro* phenotype induced by selection of human breast carcinoma cells with the chemotherapeutic drugs paclitaxel and doxorubicin. *Br J Cancer* 2004; **91**:1800–1807.

43 Perez EA. Carboplatin in combination therapy for metastatic breast cancer. *Oncologist* 2004; **9**:518–527.

44 Cocconi G, Salvagni S, Passalacqua R, Ferrozzi F, Camisa R. Design and development of new combinations of the CMF agents with taxanes (paclitaxel or docetaxel) in advanced breast cancer: a feasibility study. *Tumori* 2004; **90**:280–284.

45 Papazisis KT, Habeshaw T, Miles DW and Herceptin-EAP Study Group. Safety and efficacy of the combination of trastuzumab with docetaxel for HER2-positive women with advanced breast cancer. A review of the existing clinical trials and results of the expanded access programme in the UK. *Int J Clin Pract* 2004; **58**:581–586.

46 Fitzpatrick FA, Wheeler R. The immunopharmacology of paclitaxel (Taxol), docetaxel (Taxotere), and related agents. *Int Immunopharmacol* 2003; **3**:1699–1714.

47 Mc Gee MM, Hyland E, Campiani G, Ramunno A, Nacci V, Zisterer DM. Caspase-3 is not essential for DNA fragmentation in MCF-7 cells during apoptosis induced by the pyrrolo-1,5-benzoxazepine,PBOX-6. *FEBS Lett* 2002; **515**:66–70.

48 Buckley CD, Pilling D, Henriquez NV, Parsonage G, Threlfall K, Scheel-Toellner D, *et al.* RGD peptides induce apoptosis by direct caspase-3 activation. *Nature* 1999; **397**:479–480.

49 Klionsky DJ. *Autophagy*. Georgetown, TX: Landes Bioscience; 2004.

50 Yoshimori T. Autophagy: a regulated bulk degradation process inside cells. *Biochem Biophys Res Commun* 2004; **313**:453–458.

51 Meijer AJ, Codogno P. Regulation and role of autophagy in mammalian cells. *Int J Biochem Cell Biol* 2004; **36**:2445–2462.

52 Gozuacik D, Kimchi A. Autophagy as a cell death and tumor suppressor mechanism. *Oncogene* 2004; **23**:2891–3906.

53 Mizushima N. Methods for monitoring autophagy. *Int J Biochem Cell Biol* 2004; **36**:2491–3502.

54 Ogier-Denis E, Codogno P. Autophagy: a barrier or an adaptive response to cancer. *Biochim Biophys Acta* 2003; **1603**:113–128.